Physical Realizable Circuit Structure For Adaptive Frequency Hopf Oscillator

Arash Ahmadi Eduardo Mangieri Koushik Maharatna Mark Zwolinski
Electronic System and Devices Group
School of Electronic and Computer Science, University of Southampton, UK
Email: {aa5,em07r,km3,mz}@ece.soton.ac.uk

***Abstract*— This paper presents a novel structure for the adaptive frequency Hopf oscillator where the nonlinear function is modified to make the system realizable using analog circuit components. Mathematical model is derived and it is shown using VHDL-AMS model that despite using a new nonlinear function, the oscillator exhibits the same characteristics as the original one. Our simulation results show the same learning behavior of this oscillator with improved learning time. Subsequently, an equivalent circuit model and transistor level implementation for the oscillator is suggested and the mathematical model is confirmed with system and circuit level simulations.**

I. Introduction

Over the years the theory of Nonlinear Oscillators has been used as a mathematical tool for modeling several scientific phenomena [1]–[7]. Despite complexity of the nonlinear oscillators, their wide range of applicability has made them a serious suggestion for future generation system design in electronics [8]. Recently, in [9] Buchli et al. developed a new type of nonlinear oscillator by modifying the original Hopf oscillator where, under an additive perturbation, the intrinsic frequency of the system evolves towards the frequency of the perturbation. For nonstationary signals it works in the analogous way to wavelet or Short Time Fourier Transform (STFT), which are essential techniques in time-frequency analysis methods. The present work is motivated by this work where we look at the proposed nonlinear oscillator from a circuit design point of view.

In terms of circuit implementation, the oscillator proposed in [9] has two fundamental difficulties. Firstly, it still uses complex nonlinear functions which are extremely hard to realize in practice and secondly, the intrinsic frequency of the oscillator is considered as a system state, which in analog circuit design has to be represented as capacitor voltage (or inductance current). This linear relationship between the frequency and voltage implies that the voltage needs to be impractically high to represent a frequency greater than a few Hz meaning that the frequency basin will be too small for practical applications. These two practical problems inspire us to develop a novel circuit realizable nonlinear oscillator while staying within the framework of the same applications. Through simulations we show that the proposed function not only produces the same oscillation characteristics as the original one but also adapts the frequency at a faster rate. The second novelty of our work is that, we develop a method for extending the frequency basin significantly. Subsequently, we propose an equivalent circuit model for the entire system and validate it by circuit simulation. It is to be noted that this work is still under development and detailed mathematical proofs and complete circuit design methodology are underway. The rest of the paper is organized as follows: section II presents the background of Hopf oscillator and the modification done to it in [9] whereas the modification done in the present work is discussed in section III. The equivalent circuit structure and its simulation results and conclusion are provided in sections IV and V respectively.

II. background

The dynamics of the Hopf oscillator can be described as the following ordinary differential equations [10]:

$$\begin{aligned} \dot{x} &= \left(\mu - \left(x^2+y^2\right)\right)x + \omega y \\ \dot{y} &= \left(\mu - \left(x^2+y^2\right)\right)y - \omega x \end{aligned} \tag{1}$$

where x, y are the *states* of the oscillator and ω is the intrinsic frequency and μ determines the steady state amplitude of oscillations ($x_\infty^2+y_\infty^2=\mu$) [11]. For $\mu>0$ the origin becomes an unstable focus for the system where stable periodic solutions, namely limit cycles, are as:

$$x=\sqrt{\mu}\sin\left(\omega t+\theta_0\right), \qquad y=\sqrt{\mu}\cos\left(\omega t+\theta_0\right), \tag{2}$$

where θ_0 is determined by initial conditions. In [9], this oscillator is modified to receive an input $I(t)$, which is an additive perturbation to the $\dot{x}$ and the system intrinsic frequency ω, to evolve oscillator's frequency toward $I(t)$. This oscillator is specified as:

$$\begin{aligned} \dot{x} &= \left(\mu - \left(x^2+y^2\right)\right)x + \omega y + KI(t) \\ \dot{y} &= \left(\mu - \left(x^2+y^2\right)\right)y - \omega x \\ \dot{\omega} &= KI(t)\frac{y}{\sqrt{x^2+y^2}} \end{aligned} \tag{3}$$

where $K>0$ is a coupling constant.

Physically, in (3), x^2+y^2 can be considered as an absolute measure of the oscillation amplitude, where the term $x^2+y^2=\mu$ represents the distance from the center when the system oscillation is represented in the X-Y coordinate system. Subsequently, the term $\sin(\alpha)=\frac{y}{\sqrt{x^2+y^2}}$ represents the tangential component of the teaching force on the X-Y projection graph of the oscillation at the point $(x(t),y(t))$; more details can be found in [12]. Equation (3) induces several interesting

properties to the original Hopf oscillator as discussed in detail in [4], [9], [12]. The most interesting property is that the oscillator tries to tune its frequency to the frequency of $I(t)$. If $I(t)$ comprises different frequencies, the oscillator tunes itself to one of the frequencies depending on the initial values of the state variables and the frequency characteristics of $I(t)$. More importantly, even when $I(t)$ is withdrawn, the oscillator keeps oscillating with the frequency it was tuned to. Thus, a number of these oscillators can be employed to obtain the complete time-frequency map of $I(t)$. However, as mentioned earlier, realization of (3) is very difficult in practice particularly because of presence of the terms $\frac{y}{\sqrt{x^2+y^2}}$ and x^2+y^2. Also the linear relationship between $\dot{\omega}$ and voltage puts severe restrictions on the size of frequency basin. In the next Section we propose modifications in (3), which is easy to implement in practice and also propose a method to extend the range of the frequency basin of the oscillator.

III. Proposed Oscillator

A. Mathematical Form

In our proposed oscillator, to create the limit cycle behavior of the system, we suggest using $|x|+|y|$ as the amplitude measure which means replacing the circle $x^2+y^2=\mu$ in phase space with a square as $|x|+|y|=\sqrt{\mu}$. Consequently, as shown in Fig.1, the tangential component of the teaching force can simply be defined by $\sin(\alpha)=\frac{\sqrt{2}}{2}\cdot sgn(y)$, where $sgn(y)$ represents sign function. Applying these modifications

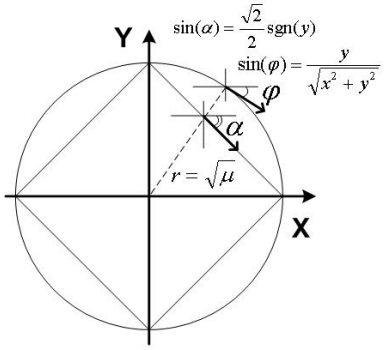

Fig. 1. Piecewise-linear approximation of the limit cycle.

to (3), the dynamics of the proposed oscillator can be given as:

$$\begin{aligned}\dot{x} &= (\mu-(|x|+|y|))\,x+\omega\cdot y+KI(t)\\ \dot{y} &= (\mu-(|x|+|y|))\,y-\omega\cdot x\\ \dot{\omega} &= KI(t)\cdot sgn(y)\end{aligned}\tag{4}$$

Note that, at circuit level the term $|x|+|y|$ can be implemented easily using full-wave rectifier and $sgn(y(t))$ is a simple comparator. However stability and frequency convergence of the system can be proved using Lyapunov method and perturbation analysis respectively, due to page restrictions, it can not be presented in this paper [10], [13]. The functional validation of the proposed oscillator described in (4) is shown in the next Subsection.

B. System Level Simulation Results

To investigate the functional behavior of the proposed oscillator, it is modeled using VHDL-AMS [14] and Mentor Graphics AdvanceMS tools. At the same time, for comparison, the oscillator proposed in [9] is also implemented using the same set of system level design tools. Investigations have been done on three particular issues, namely, rate of frequency convergence of the proposed oscillator, effect of K on the frequency convergence rate, and the tuning property of an array of different oscillators at different frequencies.

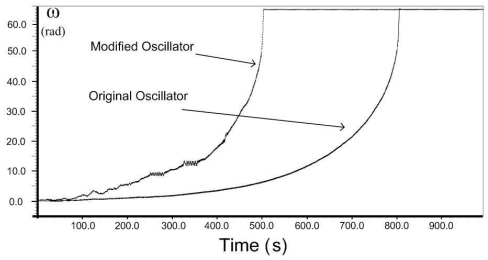

Fig. 2. Frequency convergence comparison between original oscillator of [9] and our proposed oscillator, f=10,K=10.

Fig.2 shows the frequency convergence characteristic of the proposed oscillator, comparing with the oscillator presented in [9], for a monotone input. It is observable that the modified oscillator converges to the desired frequency in a shorter time. The modified oscillator is faster because the introduced teaching force is bigger than teaching component in (3) (note that: $\text{sgn}(y)\geq\frac{y}{\sqrt{x^2+y^2}}$ for $x,y\in\mathbf{R}$). However, the convergence characteristics of the oscillator proposed in [9] is smoother than the one proposed here which shows some "roughness". We believe that this is due to the fact that the value of tangential teaching component of the adopted piecewise linear function regulating the oscillator has a fixed value for each particular region in X-Y plane. On the other hand, the same component for the nonlinear function governing the oscillator proposed in [9] adjusts itself smoothly in the phase space. However, this behavior does not affect the final value of the frequency at which the oscillator converges as shown in the Fig.2.

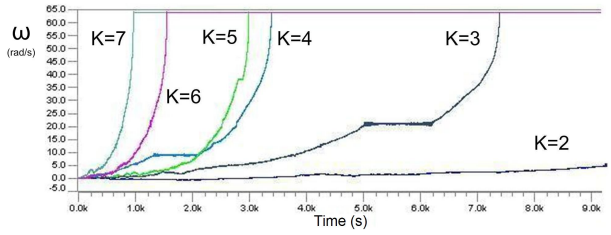

Fig. 3. Frequency convergence characteristics for different values of K (f=20π,K=2-7).

Fig.3 shows the frequency convergence characteristics of the proposed oscillator for different values of K keeping the initial values of the state variables constant. It is evident, in consistent with [9], that with increasing values of K the

oscillator converges to the desired frequency at faster rate. However, simulations show that a bigger value of K can cause oscillatory behavior in ω after convergence. Therefore a trade-off between the speed and stability has to be done for choosing the value of K under a particular circumstance. Fig.4 shows the behavior of the oscillator when the external perturbation is non-stationary. In this simulation an input signal with different frequencies and amplitudes in different times is used. As it is shown, the oscillator "learns" different frequencies of the input in different time slices. This characteristic can be employed to perform a time-frequency analysis of a non-stationary input signal by using an array of oscillators operating in different time zones. Also note that when the input signal is withdrawn, the oscillator keeps oscillating with the latest frequency it encountered in the input signal, thereby "memorizing" it.

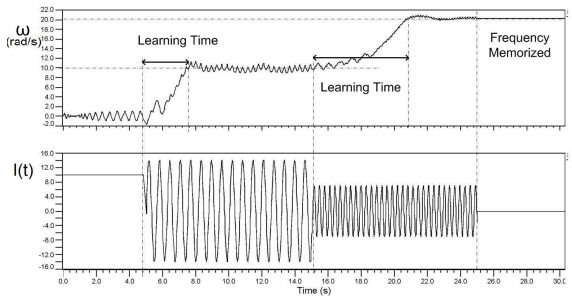

Fig. 4. Oscillator response to a non-stationary input signal.

To demonstrate the behavior of our oscillator for separating different frequency components present in a particular signal we have used an input signal composed of three frequencies, *viz*. 50, 30 and 10 Hz, each of the components having different amplitudes. We employed identical oscillators with different initial state values. The result is shown in Fig.5. In this case, each of these oscillators converges to its nearest frequency value and keeps oscillating at that frequency when the input signal is withdrawn. It is to be noted that for each of the oscillators, the choice of initial value impacts significantly on the time of frequency convergence. It also shows that each initial value inherently has a "band" of frequencies which the oscillator can converge to.

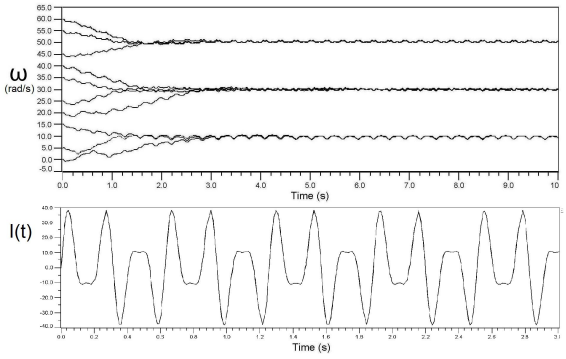

Fig. 5. An Array of similar oscillators with different initial values.

C. Extension of the Frequency Basin

As mentioned earlier, one fundamental problem of this oscillator is that due to the linear relationship between ω and the voltage representing its value, the achievable size of frequency basin is very small for practical purposes. To overcome this problem, we observe from (3),

$$\begin{aligned} \omega &= \omega_0 + \Delta\omega, \\ &= \omega_0 + K\int_0^t I(\tau)sgn(y(\tau))d\tau, \end{aligned} \tag{5}$$

Thus, we split the system frequency into two parts, ω_0 and $\Delta\omega$, where the first one is the initial value and the latter is the variable part which evolves to synchronize the oscillator with the input signal. ω_0 can be set to a value which is reasonably close to the frequency component under investigation and directly inserted in x and y state equations (see (3) and (6)) instead of ω. In this way, a spectrum analyzer can be designed using a set of oscillators in which initial values of the ω_0 are chosen equally distributed over the range of the expected spectrum of the input signal. Every oscillator in this set will catch the closest frequency component (if any) to its initial frequency (ω_0). Using this modification in (4) the final governing equation for our oscillator can be give as:

$$\begin{aligned} \dot{x} &= (\mu - (|x| + |y|))\, x + \omega_0 y + \Delta\omega \cdot y + KI(t) \\ \dot{y} &= (\mu - (|x| + |y|))\, y - \omega_0 x - \Delta\omega \cdot x \\ \dot{\Delta\omega} &= KI(t) \cdot sgn(y) \qquad with \quad \Delta\omega(0) = 0 \end{aligned} \tag{6}$$

Note that from the circuit design point of view, the terms $\omega_0 x$ and $\omega_0 y$ are actually amplification rather than multiplication. In other words, it can be considered as a conventional oscillator with a fixed amplitude (μ) and frequency (ω_0), where the oscillation frequency is tunable within the range of $\omega_0 \pm \Delta\omega$ and $\Delta\omega$ is governed by the third state equation in (6).

IV. Circuit Implementation

A. Circuit Model and Implementation

Fig.6-I shows the equivalent circuit model of the oscillator using basic circuit elements where the system states are represented as capacitance voltages. Considering explanations of the last paragraph of Section III-C, this model consists of two major sections: traditional oscillator and adaptation circuit, where the first one creates a limited-amplitude oscillation and the latter one controls $\Delta\omega$ to adapt the frequency. A transistor level implementation of this structure is presented in Fig.6-II, where role of each section of the circuit is also denoted, more details regarding circuit can be found in [15].

B. Simulation Results

Specified circuit in Fig.6 simulated in Cadence Spectre utilizing 0.12 μm technology and dual ended supply with value 0.6 V. A full set of simulations are performed to evaluate circuit capabilities and here we present two important results due to space restrictions. Fig.8 shows response of the circuit to monotone sinusoidal inputs as ω_1=40MHz, ω_2=30MHz and ω_3=20MHz with amplitude of 300mV. It can be observed that

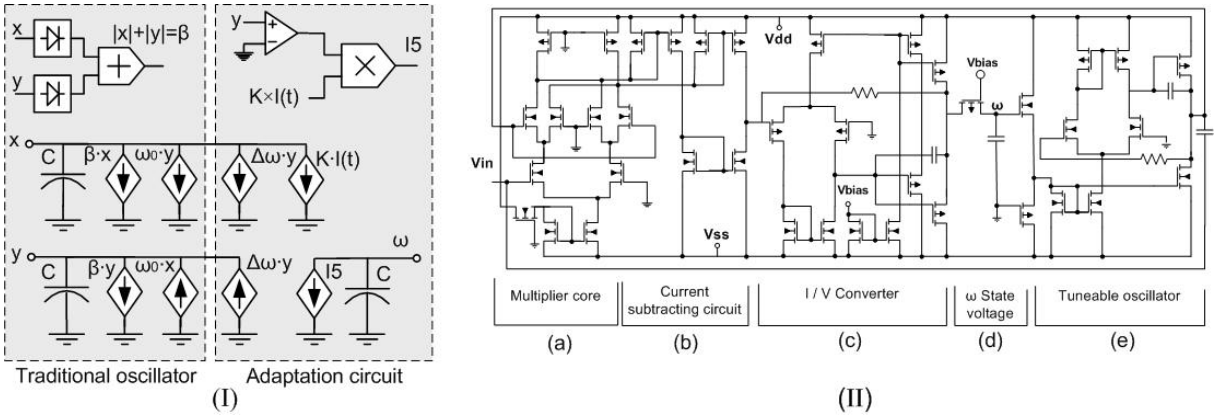

Fig. 6. Circuit implementation using traditional circuit elemnts I)Block diagram of the equivalent circuit II)Transistor level implementation of the system.

the behavior of the oscillator is consistent with the system level simulations. To examine the circuit response to non-stationary signals consider Fig.8, where an input signal with different frequencies in different time durations is applied. As it can be observed from simulation result, oscillator adapts its frequency to the new input frequencies in each period of time. Unlike system level simulations here and in [9], learning times are very short and even negligible with this design methodology.

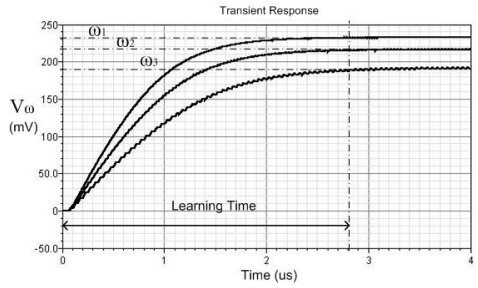

Fig. 7. Simulation results for different input frequencies.

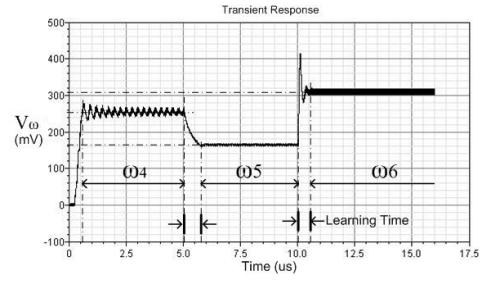

Fig. 8. Oscillator response to a non-stationary monotone ($\omega_5 < \omega_4 < \omega_6$).

V. Conclusion

This paper presents a new nonlinear oscillator, which has the same characteristics of the adaptive frequency Hopf oscillator but at the same time can be implemented in real life for a larger frequency basin. Our system level simulation results show that not only this oscillator learns the frequency of the input signal but also does so in a shorter time. The simulation results for the circuit shows complete consistency with the mathematical model as well as system level simulations. These results imply that it is possible to employ the proposed oscillator for performing a wide range of signal processing tasks in real life.

References

[1] E. Izhikevich and Y. Kuramoto, *Encyclopedia Of Mathematical Physics*. ACADEMIC PRESS, 2006, ch. Weakly Coupled Oscillators, p. 5:448.

[2] K. Chen and D. Wang, "A dynamically coupled neural oscillator network for image segmentation," *Neural Networks*, vol. 15, no. 3, pp. 423–439, April 2002.

[3] C. M. Pinto and M. Golubitsky, "Central pattern generators for bipedal locomotion," *Journal of Mathematical Biology*, vol. 53, no. 3, pp. 474–489, September 2006.

[4] J. Buchli and A. J. Ijspeert, "A simple, adaptive locomotion toy-system," in *In Proceedings SAB04*. MIT Press, 2004, pp. 153–162.

[5] L. Chua and T. Roska, *cellular neural networks and visual computing: foundations and applications*. cambridge university press, 2005.

[6] I. Szatmri and L. O. Chua, "Awakening dynamics via passive coupling and synchronization mechanism in oscillatory cellular neural/nonlinear networks," *International Journal of Circuit Theory and Applications*, vol. 36, no. 5-6, pp. 525 – 553, June 2008.

[7] D. Xu, J. C. Principe, and J. G. Harris, "Logic computation using coupled neural oscillators," in *International Symposium on Circuits and Systems (ISCAS)*, vol. 5. IEEE, May 2004, pp. V–788 – V–791.

[8] N. R. Shanbhag, S. Mitra, G. de Veciana, M. Orshansky, R. Marculescu, J. Roychowdhury, D. Jones, and J. M. Rabaey, "The search for alternative computational paradigms," *IEEE Design & Test of Computers*, vol. 25, no. 4, pp. 334 – 343, July-August 2008.

[9] J. Buchli, L. Righetti, and A. J. Ijspeert, "Frequency analysis with coupled nonlinear oscillators," *Physica D: Nonlinear Phenomena*, vol. 237, no. 13, pp. 1705–1718, August 2008.

[10] P. G. Drazin, *Nonlinear Systems (Cambridge Texts in Applied Mathematics)*. Cambridge University Press, Jan 2008.

[11] A. I. Mees and L. . Chua, "The Hopf bifurcation theorem and its applications to nonlinear oscillations in circuits and systems," *IEEE Transactions on Circuits and Systems*, vol. 26, no. 4, pp. 235– 254, April 1979.

[12] L. Righetti, J. Buchli, and A. J. Ijspeert, "Dynamic hebbian learning in adaptive frequency oscillators," *Physica D: Nonlinear Phenomena*, vol. 216, no. 2, pp. 269–281, 2006.

[13] H. K. Khalil, *Nonlinear Systems*, 3rd ed. Prentice Hall, Jan 2002.

[14] P. J. Ashenden, G. D. Peterson, and D. A. Teegarden, *The System Designer's Guide to VHDL-AMS: Analog, Mixed-Signal, and Mixed-Technology Modeling (Systems on Silicon)*. Morgan Kaufmann, September 2003.

[15] E. Mangieri, A. Ahmadi, K. Maharatna, S. Ahmad, and P. Chappell, "A novel analogue circuit for controlling prosthetic hands," in *IEEE Biomedical Circuits and Systems Conference*, vol. 1, November 2008, pp. 81–84.